SWITCHING OBSERVER DESIGN FOR AN EXPERIMENTAL PIECE-WISE LINEAR BEAM SYSTEM [1]

A. Doris [*] **A.Lj. Juloski** [**] **W.P.M.H. Heemels** [***]
N. van de Wouw [*] **H. Nijmeijer** [*]

[*] *Department of Mechanical Engineering*
Eindhoven University of Technology
P.O. Box 513, NL 5600 MB Eindhoven
The Netherlands
Email: a.doris@tue.nl, N.v.d.Wouw@tue.nl, h.nijmeijer@tue.nl
[**] *Department of Electrical Engineering*
Eindhoven University of Technology
P.O. Box 513, MB 5600 MB Eindhoven
The Netherlands
Email: a.juloski@tue.nl
[***] *Embedded Systems Institute*
P.O. Box 513, MB 5600 MB Eindhoven
The Netherlands
Email: maurice.heemels@embeddedsystems.nl

Abstract: This paper presents an implementation of a switching observer design strategy to a piece-wise linear beam system comprising a flexible steel beam with a one-sided support. The switching observer design strategy guarantees asymptotic stability of the estimation error. Experimental and simulation results are presented to demonstrate the observer error stability and performance.

1. INTRODUCTION

This paper presents an experimental study of a switching observer design strategy for a class of piece-wise linear systems by application to an elastic beam with a one-sided support. The experimental beam system consists of a flexible steel beam, which is clamped on two sides and is supported at a location by a one-sided linear spring. Due to the one-sided spring the beam has two different dynamical regimes, which can be both be well described as linear. As such the beam system can be represented by a bi-modal piece-wise linear system. The mechanical motivation to study such a piece-wise linear beam system is the analysis of the dynamics of complicated engineering constructions, such as tower cranes, suspension bridges and solar panels on satellites which exhibit structural elements with piece-wise linear restoring characteristics, see (Heertjes, 1999).

For this experimental beam we will design a switching observer using the strategy from (Juloski *et al.*, 2002). In (Juloski *et al.*, 2002) observers of Luenberger type are considered, which result for a bi-modal piece-wise linear system like the beam in bi-modal piece-wise linear observers. It is a distinguishing feature of this observer structure that the observer does not need information about the active dynamics of the system, in contrast to observers proposed in (Alessandri and Colleta, 2001*a*) and (Alessandri and Colleta, 2001*b*). The observer design strategy focuses on the state estimation error dynamics defined by interconnecting a bi-modal piece-wise linear system with a bi-modal piece-wise linear observer. Contrary to the classical Luenberger observer for linear systems and to the case

[1] Supported by European project SICONOS (*IST* – 2001 – 37172)

when the mode is known, in this case the error dynamics is not autonomous, but depends on the state of the observed system, and is a piece-wise linear system with four modes. The theory of (Juloski *et al.*, 2002) gives conditions under which global asymptotic stability of the estimation error is achieved. These conditions imply that the bi-modal system at hand should be continuous over the switching plane. This is the case for the piece-wise linear model of the beam system. By suitably selecting the output variable of the beam system a piece-wise linear observer can be designed for the model of the piece-wise linear set-up.

The focus of the paper is on the implementation of this piece-wise linear observer for the experimental beam system and on the comparison of the observer predictions with simulations and experimental measurements.

The paper is structured as follows. The switching observer design strategy is introduced in section 2. In section 3, a description of the experimental beam system is given. The modelling of the beam system and a model reduction method are discussed in section 4. In sections 5 and 6, simulation and experimental results related to the observer performance are presented. Conclusions and future work are given in section 7.

2. SWITCHING OBSERVER DESIGN

We consider a continuous-time bi-modal piece-wise linear system of the following type:

$$\dot{x}(t) = \begin{cases} A_1 x(t) + Bu(t), \text{ if } H^T x(t) \leq 0 \\ A_2 x(t) + Bu(t), \text{ if } H^T x(t) > 0 \end{cases} \tag{1a}$$

$$y(t) = C\,x(t), \tag{1b}$$

where $x(t) \in \mathbb{R}^n, y(t) \in \mathbb{R}^p$ and $u(t) \in \mathbb{R}^m$ are the state, output and the input of the system, respectively, at time $t \in [0, \infty)$. The matrices $A_1, A_2 \in \mathbb{R}^{n\times n}$, $B \in \mathbb{R}^{n\times m}$, $C \in \mathbb{R}^{p\times n}$ and $H \in \mathbb{R}^n$. The hyperplane defined by $\ker H^T$ separates the state space $\mathbb{R}^n$ into the two half-spaces. The vector-fields of (1a) coincide on the half-space boundary ($A_1 = A_2$ if $H^T x = 0$). The considered class of piece-wise linear systems has an identical input matrix B and an identical output matrix C for both modes. The problem at hand is to design a state estimation procedure, which, on the basis of the known system model, input u, and measured output y provides a state estimate $\hat{x}$, without directly measuring which mode of the system is active. In order to do so, we choose an observer for the system (1), with the following structure:

$$\dot{\hat{x}}(t) = \begin{cases} A_1 \hat{x}(t) + Bu(t) + L_1 \Delta y(t), \text{ if } H^T \hat{x}(t) \leq 0 \\ A_2 \hat{x}(t) + Bu(t) + L_2 \Delta y(t), \text{ if } H^T \hat{x}(t) > 0 \end{cases} \tag{2a}$$

$$\hat{y}(t) = C\,\hat{x}(t), \tag{2b}$$

where $\hat{x}(t) \in \mathbb{R}^n$ is the estimated state at time t, $L_1, L_2 \in \mathbb{R}^{n\times p}$ and $\Delta y(t) = y(t) - \hat{y}(t)$. Consequently, the dynamics of the state estimation error $e = x - \hat{x}$ is described by

$$\dot{e} = \begin{cases} (A_1 - L_1 C)e, & H^T x \leq 0,\ H^T \hat{x} \leq 0 \\ (A_2 - L_2 C)e + \Delta A x, & H^T x \leq 0,\ H^T \hat{x} > 0 \\ (A_1 - L_1 C)e - \Delta A x, & H^T x > 0,\ H^T \hat{x} \leq 0 \\ (A_2 - L_2 C)e, & H^T x > 0,\ H^T \hat{x} > 0, \end{cases} \tag{3}$$

where $\Delta A = A_1 - A_2$, x satisfies (1a) and $\hat{x}$ satisfies (2a). By substituting $\hat{x} = x - e$ in (3), we see that the right-hand side of the state estimation error dynamics is piece-wise linear in the variable $[e \quad x]^T$.

In (Juloski *et al.*, 2002) the observer design problem was formally stated as follows.

Problem: *Determine, if possible, observer gains L_1, L_2 and K in* (2a) *such that global asymptotic stability of the estimation error dynamics* (3) *is achieved, for all functions $x : \mathbb{R}^+ \longrightarrow \mathbb{R}^n$, satisfying* (1) *for some given $u : \mathbb{R}^+ \longrightarrow \mathbb{R}^m$.*

Theorem 1. The state estimation error dynamics (3) is globally asymptotically stable for all $x : \mathbb{R}^+ \longrightarrow \mathbb{R}^n$ satisfy (1) for some locally integrable input function $u : \mathbb{R}^+ \longrightarrow \mathbb{R}^m$ (in the sense of Lyapunov), if there exist matrices $P = P^T > 0$, L_1, L_2 and constants $\lambda_1, \lambda_2 \geq 0$, $\mu > 0$ such that the following set of matrix inequalities is satisfied:

$$\begin{bmatrix} (A_2 - L_2C)^T P & P\Delta A \\ +P(A_2 - L_2C) + \mu I & +\lambda_1 \frac{1}{2} HH^T \\ \Delta A^T P & -\lambda_1 HH^T \\ +\lambda_1 \frac{1}{2} HH^T & \end{bmatrix} \leq 0 \tag{4a}$$

$$\begin{bmatrix} (A_1 - L_1C)^T P & -P\Delta A \\ +P(A_1 - L_1C) + \mu I & +\lambda_2 \frac{1}{2} HH^T \\ -\Delta A^T P & -\lambda_2 HH^T \\ +\lambda_2 \frac{1}{2} HH^T & \end{bmatrix} \leq 0 \tag{4b}$$

For the proof of *Theorem 1* the reader is referred to (Juloski *et al.*, 2002).

Remark 2.1 The observer does not require information on which linear dynamics of the system is currently active, due to its switching structure.

Remark 2.2 The inequalities (4a)-(4b) are nonlinear matrix inequalities in $\{P, L_1, L_2, \lambda_1, \lambda_2, \mu\}$, but are linear in $\{P, L_1^T P, L_2^T P, \lambda_1, \lambda_2, \mu\}$, and thus can be efficiently solved using linear matrix inequalities solvers (such as the software LMItool for Matlab).

Remark 2.3 A necessary condition for the LMIs (4) to be feasible is

$$P = P^T > 0 \tag{5a}$$

$$(A_1 - L_1C)^T P + P(A_1 - L_1C) < 0 \tag{5b}$$

$$(A_2 - L_2C)^T P + P(A_2 - L_2C) < 0. \tag{5c}$$

Based on (Alessandri and Colleta, 2001*a*), (Alessandri and Colleta, 2001*b*) these inequalities imply that the pairs (A_1, C) and (A_2, C) are detectable as linear systems in the standard sense. Hence, a necessary condition for the observer design, using (4), to work is detectability of the two linear subsystems in the usual sense.

3. EXPERIMENTAL BEAM SYSTEM

The experimental set-up [2] (see Figures 1 and 2) consists of a steel beam supported at both ends by two leaf springs. The beam is excited by a force u generated from a rotating mass-unbalance, which is mounted at the middle of the beam. A tacho-controlled motor, that enables a constant rotation speed, drives the mass-unbalance. A second beam, that is clamped at both ends, is located parallel to the first one and acts as a one-sided spring. This one-sided spring represents a non-smooth nonlinearity in the dynamics of the steel beam and, as a result, the beam system (beam and one-sided spring) has nonlinear and non-smooth dynamics. In case the spring is linear, the beam system can be described as a piece-wise linear system, as we will show in the next section. For further information on the experimental set-up the reader is referred to (Van der Vorst, 1996) and (Heertjes, 1999).

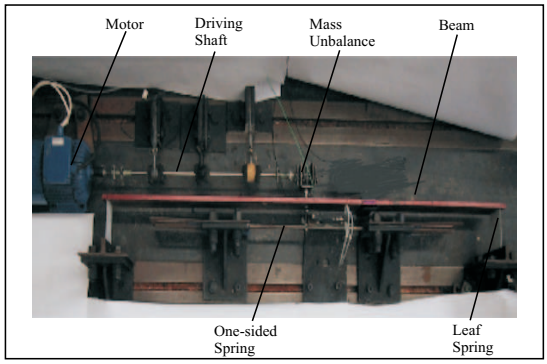

Fig. 1. Photo of the experimental set-up.

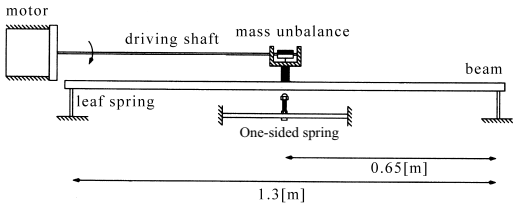

Fig. 2. Schematic view of the experimental set-up.

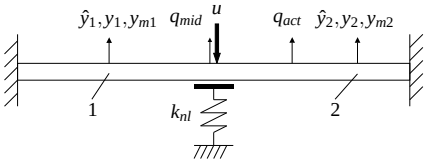

Fig. 3. Elastic beam with one-sided support.

4. MODELLING

When the beam moves from its rest point towards the one-sided spring, the spring is active. Therefore, the system has different dynamics on this side than on the opposite side. In the first case, the system dynamics is determined by the stiffness of the beam and the spring, in the second case, only by the beam stiffness. The switching boundary between the two dynamic regimes is present at zero displacement of the middle of the beam. In order to describe the behavior of the beam accurately, a 111DOF finite element model has been developed, see (Bonsel *et al.*, 2004). Due to the large number of the model DOFs , the simulation of the nonlinear responses is computationally expensive. In addition to that, the solution of the LMIs (4) is very complex for such high order systems. Therefore, a dynamic component mode synthesis reduction method is used to express the number of DOF of the FEM in terms of a reduced set of DOF. We use the so-called Rubin method (Craig, 1985). The product of this reduction is a 3DOF model. The relation between the DOF of the FEM and the reduced model is given with

$$p = Tq, \tag{6}$$

where p denotes the DOFs of the FEM model and q the DOFs of the reduced model. The transformation matrix $T \in \mathbb{R}^{111\times 3}$ obtained from the model reduction procedure has the following structure:

$$T = [\tau_1 \mid \tau_2 \mid \cdots \mid \tau_{111}]^T, \tag{7}$$

where $\tau_i \in \mathbb{R}^3$. For further details of the reduction method the reader is referred to (Fey, 1992) and (Bonsel *et al.*, 2004). The dynamics of the system described by the 3DOF model is

$$M\ddot{q} + B\dot{q} + Kq + f_{nl}(q) = h\,u(t), \tag{8}$$

where $h = [1 \quad 0 \quad 0]^T$ and $q = [q_{mid} \quad q_{act} \quad q_\xi]^T$. Herein, q_{mid} is the displacement of the middle of the beam and q_{act} is the displacement of a point depicted in Figure 3. Moreover, q_ξ reflects the contribution of the first eigenmode of the beam and M, B and K are the mass, the damping and the stiffness matrices of the reduced model, respectively. We apply a periodic excitation force

$$u(t) = A\sin\omega t, \tag{9}$$

which is generated by the mass-unbalance at the middle of the beam. Herein, ω is the excitation frequency and A the amplitude of the excitation force. Moreover, f_{nl} is the restoring force of the one-sided spring:

$$f_{nl}(q) = k_{nl}\,h\,min(0, h^T q) = k_{nl}\,h\,min(0, q_{mid}), \tag{10}$$

where k_{nl} is the stiffness of the spring. The force f_{nl} acts when there is a contact between the middle of the beam and the one-sided spring.

In state-space form, the model takes the form of (1), where $x = [q^T \quad \dot{q}^T]^T$, $H = [h^T \quad 0^T]$, $0 = [0 \quad 0 \quad 0]^T$,

$$A_1 = \begin{bmatrix} 0 & I \\ -M^{-1}(K + k_{nl}\,h\,h^T) & -M^{-1}B \end{bmatrix},$$

$$A_2 = \begin{bmatrix} 0 & I \\ -M^{-1}K & -M^{-1}B \end{bmatrix},$$

$$B = \begin{bmatrix} 0 \\ M^{-1}h \end{bmatrix}.$$

The numerical values of these matrices are given in Appendix.

Remark 4.1 Note that the output y of the model is the displacement of a point along the beam. A detailed description of y for the examined system is

$$y = p_i = \tau_i q = [\,\tau_i^T \quad 0^T]x = Cx, \tag{11}$$

[2] Available in the Dynamics and Control Technology laboratory of the Mechanical Engineering Department of the Eindhoven University of Technology

where p_i is the $i-th$ DOF of the 111DOF model, τ_i is the $i-th$ row of the transformation matrix T, 0 is a zero-column of length 3 and $C = [\tau_i^T \quad 0]$ is the model output matrix for this system as in (1b).

Remark 4.2 For the examined system the hyperplane where the model switches dynamics is the rest position of the middle of the beam $H^T x = q_{mid} = 0$.

5. OBSERVER DESIGN FOR THE BEAM SYSTEM

In order to design the observer (2a) for the examined system, the transversal displacement of a properly chosen point on the beam is used as observer output injection. This displacement is described from the model output (11). The position of this point should be chosen such that both pairs (A_1, C) and (A_2, C) are detectable as linear systems, see Remark 2.3.

6. SIMULATION RESULTS

In order to validate the observer performance using simulations, the procedure depicted in figure 7 is followed. Herein, two model-based signals (y_1, y_2) that describe the displacements of two points along the beam (point 1 and 2 in figure 3, respectively) are obtained by means of simulations.

$$y_1 = C_1 x \tag{12}$$

$$y_2 = C_2 x, \tag{13}$$

where y_1 and y_2 are the $35th$- and $68th$-DOF of the 111DOF model, respectively. Therefore, $C_1 = [\tau_{35}^T \quad 0^T]$ $(i = 35)$ and $C_2 = [\tau_{68}^T \quad 0^T]$ $(i = 68)$, according to (11). Using y_1 for observer output injection, the observer reconstructs the full state $(\hat{x})$ and consequently the displacement $(\hat{y}_2 = C_2\hat{x})$ of the second point. The comparison of y_2 and $\hat{y}_2$ can be used to assess the performance of the observer.

Remark 5.1 By solving the LMIs (4a)-(4b) the gains L_1, L_2 are calculated. The numerical values of these gains, that guarantee global asymptotic stability of the state estimation error of the beam system are shown in the Appendix.

In figures 5 and 6 the displacement y_2 is compared with the $\hat{y}_2$ for different excitation frequencies ω and different amplitudes A. Furthermore, the error $e_o = \hat{y}_2 - y_2$ (observer error) is depicted in the same figures. The model and observer initial conditions x_0, $\hat{x}_0$ are shown in the Appendix. Both figures show that the observer error converges to zero , as guaranteed by the theory.

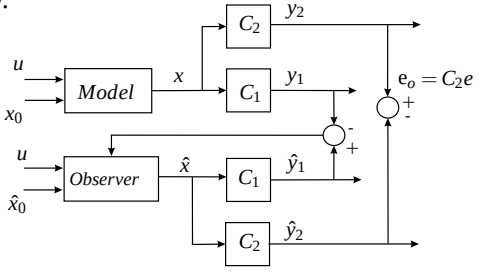

Fig. 4. Schematic representation of the procedure followed for the validation of the observer performance, based on simulations.

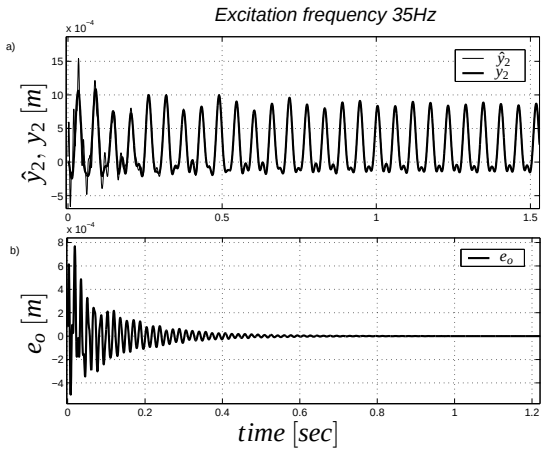

Fig. 5. a) Model prediction y_2 and observer prediction $\hat{y}_2$, b) observer error e_o for $\frac{\omega}{2\pi} = 35\ Hz$ and $A = 50\ N$.

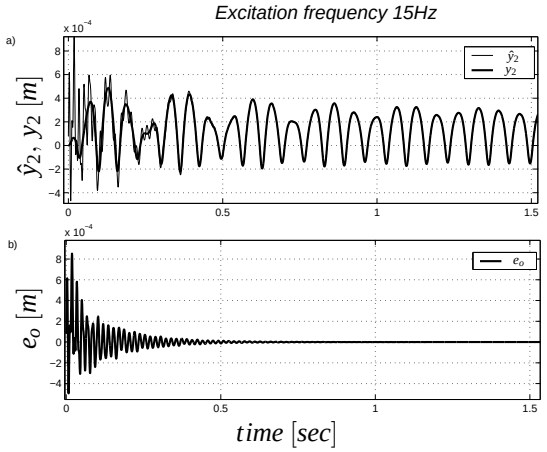

Fig. 6. a) Model prediction y_2 and observer prediction $\hat{y}_2$, b) observer error e_o for $\frac{\omega}{2\pi} = 15\ Hz$ and $A = 12\ N$.

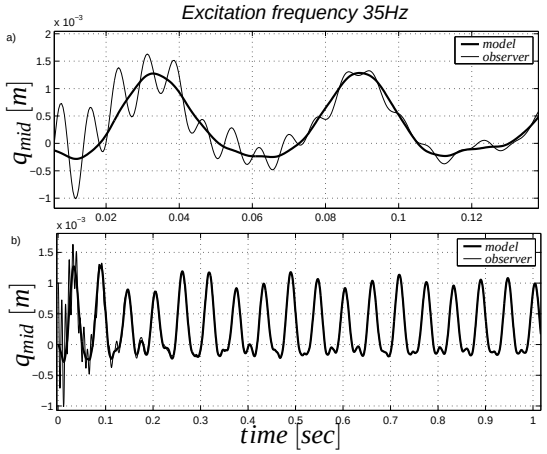

Fig. 7. Displacement q_{mid} of the middle of the beam for $\frac{\omega}{2\pi} = 35\ Hz$ and $A = 50N$. The plot a) is a zoomed version of b).

In Figure 7 the model and observer estimations of the displacement of the middle of the beam are depicted. In Figure 7a) it is shown that the model and the observer do not switch dynamics simultaneously. Nevertheless, both converge to the same steady-state solution, as can be seen in Figure 7b).

Remark 5.2 The steady-state solution of the displacements y_2 and $\hat{y}_2$ for an excitation frequency of 35 Hz is a $\frac{1}{2}$ subharmonic solution (Figures 5 and 7), while for an excitation frequency of 15 Hz it is a harmonic solution (Figure 6), see (Heertjes, 1999).

7. EXPERIMENTAL RESULTS

In order to validate the observer performance using experimental results, a comparison between the measured displacement (y_{m2}) of a point along the beam (point 2 in figure 3) with the corresponding model and observer estimations ($y_2, \hat{y}_2$) is performed. The experimental procedure followed in this case is similar to the simulation procedure. The only difference, of course, is that the output injection used here is the measured displacement (y_{m1}) of the point 1 (see figure 3). This procedure is explained in figure 8. In figures 9 to 12 the displacement estimations y_2 and $\hat{y}_2$ of the point 2, are compared with the measured displacement y_{m2} of the same point. Furthermore, the errors $e_o = \hat{y}_2 - y_{m2}$ (observer error) and $e_m = y_2 - y_{m2}$ (model error) are depicted in the same figures. The model and observer initial conditions x_0, $\hat{x}_0$ are shown in the Appendix.

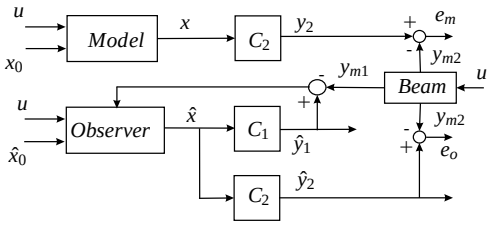

Fig. 8. Schematic representation of the procedure followed for the validation of the observer performance, based on experimental results.

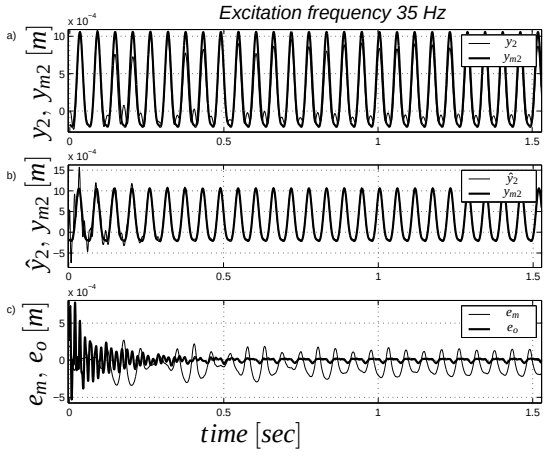

Fig. 9. Comparison of a) the measured displacement y_{m2} with the model prediction y_2, b) the measured displacement y_{m2} with the observer prediction $\hat{y}_2$ and c) the observer error e_o with the model error e_m for $\frac{\omega}{2\pi} = 35Hz$ and $A = 50\ N$.

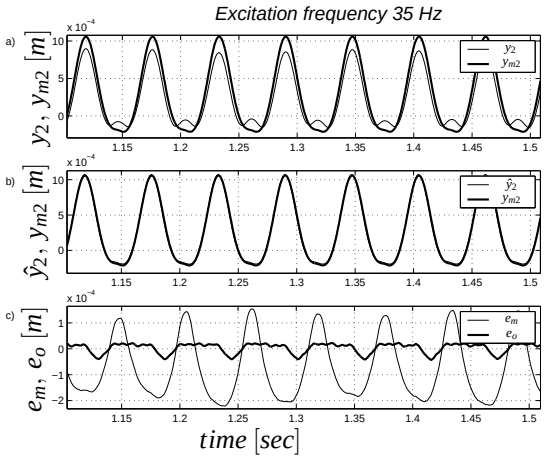

Fig. 10. Zoomed version of figure 9 in steady-state.

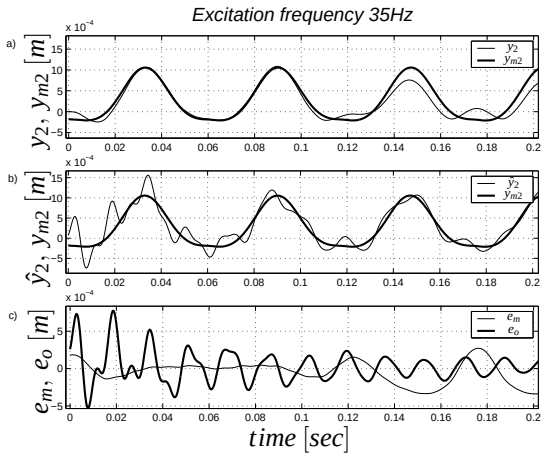

Fig. 11. Zoomed version of figure 9 in the transition-state.

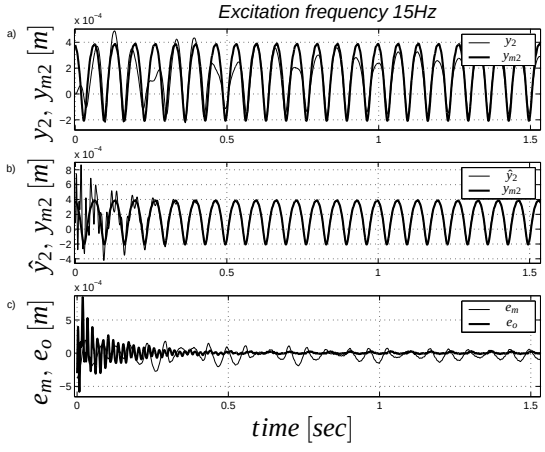

Fig. 12. Comparison of a) the measured displacement y_{m2} with the model prediction y_2, b) the measured displacement y_{m2} with the observer prediction $\hat{y}_2$ and c) the observer error e_o with the model error e_m for $\frac{\omega}{2\pi} = 15\ Hz$ and $A = 12\ N$.

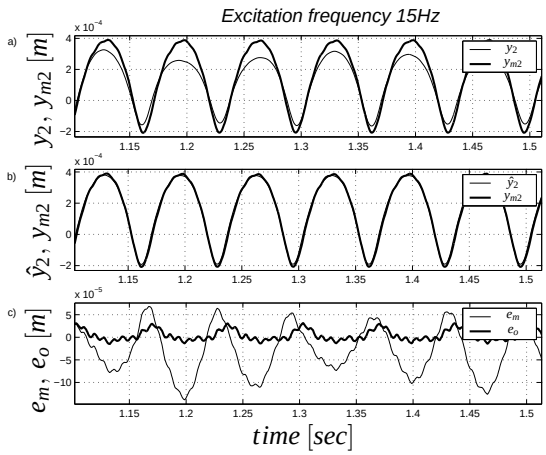

Fig. 13. Zoomed version of figure 11.

A difference between y_{m2} and y_2 exists (Figures 10 and 13) due to a model mismatch (mainly in the non-linearity related to the one-sided spring stiffness) and due to noise in the measured signals. Since the observer is a model-based observer, the error e_o will also be affected. Nevertheless, the observer performance is satisfactory, since e_o is considerably smaller than e_m in both frequencies. For an excitation frequency of 15 Hz (Figures 12 and 13), the maximum value of e_o in steady-state is around 7% of the maximum value of y_{m2}, while in 35 Hz (Figures 9 and 10), it is less than 4%. On the other hand, the maximum values of e_m at the same frequencies are above 12% of the maximum value of y_{m2}. Finally, it is worth mentioning that the error e_o converges to its steady-state solution in less than 0.4 *sec*, while e_m requires more than 1.2 *sec* for the same result.

8. CONCLUSIONS AND FUTURE WORK

A switching observer strategy is applied to a periodically excited beam with a one-sided support. The performance of the observer is shown based on both simulation and experimental results. According to these results the observer performs well, since it predicts with high accuracy the real system responses, despite the fact that there are unavoidable modelling inaccuracies and noise in the measured signals. Although the observer error e_o does not converge to zero exactly using the experimental results, it becomes clear that it is much smaller than the model error e_m for all excitation frequencies. Moreover, the observer cancels the error in the initial conditions between the model and the piece-wise linear system and forces the observer response to converge to its steady-state solution faster than the model response.

A topic of future research is the design of a controller for non-smooth switching systems based on the implemented observer and the application of this controller to the piece-wise linear beam system.

9. APPENDIX

The matrices M, K, B, L_1, L_2, C_1, C_2, x_0, $\hat{x}_0$ and the value of k_{nl} are

$$M = \begin{bmatrix} 4.494 & -2.326 & 0.871 \\ -2.326 & 7.618 & 2.229 \\ 0.871 & 2.229 & 2.374 \end{bmatrix},$$

$$K = 10^6 \begin{bmatrix} 2.528 & -0.345 & 1.026 \\ -0.345 & 1.051 & 0.296 \\ 1.026 & 0.296 & 0.613 \end{bmatrix},$$

$$B = 10^2 \begin{bmatrix} 1.173 & -0.298 & 0.416 \\ -0.298 & 1.041 & 0.314 \\ 0.416 & 0.314 & 0.365 \end{bmatrix},$$

$L_1 = 10^4 \cdot [0.0134 \quad 0.0145 \quad -0.0353 \quad 0.5402 \quad 0.9448 \quad -2.6460]$,

$L_2 = 10^4 \cdot [0.0134 \quad 0.0145 \quad -0.0353 \quad 0.7989 \quad 1.0893 \quad -2.8705]$,

$C_1 = [-0.9579 \quad 1.2165 \quad -0.2642 \quad 0 \quad 0 \quad 0]$,

$C_2 = [0.0801 \quad -1.2013 \quad -0.8669 \quad 0 \quad 0 \quad 0]$,

$x_0 = [0 \quad 0 \quad 0 \quad 0 \quad 0 \quad 0]^T$, $\hat{x}_0 = [10^{-3} \quad 0 \quad 0 \quad 0 \quad 0 \quad 0]^T$ and $k_{nl} = 198000\, N/m$.

REFERENCES

Alessandri, A. and P. Colleta (2001*a*). Design of Luenberger observers for a class of hybrid systems. *Proc. of Hybrid Systems: Computation and Control, Rome*.

Alessandri, A. and P. Colleta (2001*b*). Switching observers for continious-time and discrete-time linear systems. *Proc. of the American Control Conference* pp. 2516–2521.

Bonsel, J.H., R.H.B. Fey and H. Nijmeijer (2004). Application of a dynamic vibration absorber to a piecewise linear beam system. *Nonlinear Dynamics* pp. 227–243.

Craig, Jr, R.R. (1985). A review of time-domain and frequency-domain component mode synthesis methodes, combined experimental/analytical modeling of dynamic structural systems using substructure synthesis. *ASME Applied Mechanics AMD-67, New York* pp. 1–31.

Fey, R.H.B. (1992). Steady-state behaviour of reduced dynamics with local nonlinearities. *PhD thesis, Eindhoven University of Technology*.

Heertjes, M.F. (1999). Controlled stabilization of long-term solutions in a piece-wise linear beam system. *PhD thesis, Eindhoven University of Technology*.

Juloski, A.Lj., W.P.M.H. Heemels and S. Weiland (2002). Observer design for a class of piece-wise affine systems. *Proc. of the 41st IEEE Conference: Decision and Control, Las Vegas, Nevada, USA*. pp. 123–126.

Van der Vorst, E.L.B. (1996). Long terms dynamics and stabilization of nonlinear mechanical systems. *PhD thesis, Eindhoven University of Technology*.